# Sustainable Polymerizations in Recoverable Microemulsions

**ARTICLE** *in* LANGMUIR · FEBRUARY 2010

Impact Factor: 4.46 · DOI: 10.1021/la100502x · Source: PubMed

Langmuir
Letter
pubs.acs.org/Langmuir


# Sustainable Polymerizations in Recoverable Microemulsions

Zhenzhen Chen,[†] Feng Yan,*[,†,‡] Lihua Qiu,[†] Jianmei Lu,[†] Yinxia Zhou,[†] Jiaxin Chen,[†] Yishan Tang,[†] and John Texter*[,§]

[†]*Key Laboratory of Organic Synthesis of Jiangsu Province, School of Chemistry and Chemical Engineering, and* [‡]*Jiangsu Key Laboratory for Carbon-Based Functional Materials & Devices, Soochow University, Suzhou 215123, PR China, and* [§]*School of Engineering Technology, Eastern Michigan University, Ypsilanti, Michigan 48197*

*Received February 2, 2010. Revised Manuscript Received February 14, 2010*

Free radical and atom-transfer radical polymerizations were conducted in monomer/ionic liquid microemulsions. After the polymerization and isolation of the resultant polymers, the mixture of the catalyst and ionic liquids (surfactant and continuous phase) can be recovered and reused, thereby dramatically improving the environmental sustainability of such chemical processing. The addition of monomer to recovered ionic liquid mixtures regenerates transparent, stable microemulsions that are ready for the next polymerization cycle upon addition of initiator. The method combines the advantages of IL recycling and microemulsion polymerization and minimizes environmental disposable effects from surfactants and heavy metal ions.

Since the early 1980s, microemulsion polymerization has developed as an important methodology for the synthesis of latexes and nanostructured polymers (gels or porous polymers).[1] In addition to conventional free radical polymerization, controlled/living radical polymerization[2] including nitroxide-mediated radical polymerization (NMP),[3] reversible addition−fragmentation chain transfer (RAFT),[4] iodine-transfer polymerization (ITP),[5] and atom-transfer radical polymerization (ATRP)[6] in microemulsions have been recently developed. For example, Matyjaszewski[6a,6b] and Okubo[6c,6d] reported ATRP in aqueous microemulsions. The polymer nanoparticles produced had halide-terminal-group-functionalized surfaces suitable for further chain extension and the synthesis of core−shell, multilayered, and hairy nanoparticles. However, a limitation of microemulsion ATRP is that a high concentration of a transition-metal catalyst is generally required and these catalysts are easily coprecipitated with the polymer as contaminants and may color and even make the polymers toxic. Methods including adsorbent column, precipitation, and dialysis have been applied for the removal of residual catalyst.[7] These methods are efficient on the laboratory scale, but they become too expensive or unfeasible for large-scale industrial production. In addition, microemulsion polymerization systems usually require a high concentration of surfactant to stabilize a relatively small amount of monomer, which makes the workup very tedious when trying to purify the resulting polymers.[1] Therefore, the development of an efficient, economical method to recover and reuse both the catalysts and surfactants is very important to improve the sustainability of polymer production via microemulsion ATRP.

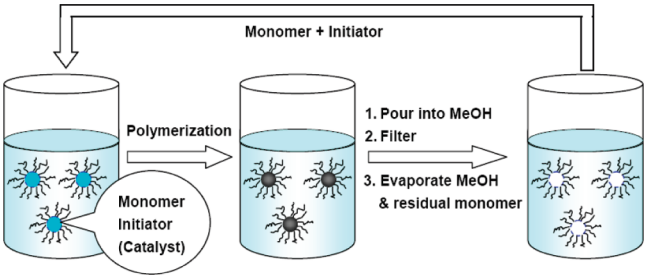


**Figure 1.** Polymerization procedures in an IL-based microemulsion.

Ionic liquids (ILs) are organic salts with melting points below 100 °C and often near or below room temperature. IL-based microemulsions have recently attracted a great deal of interest because of the unique features of both ILs and microemulsions. These IL-based microemulsions exhibit behavior consistent with "classic" aqueous microemulsions and provide nanosized IL reactors.[8] Herein, we report the first results of polymerizations conducted in monomer oil/ionic liquid microemulsions. After polymerization and isolation of the resulting polymers, the mixture of surfactant, IL, and catalyst (for ATRP) is recovered and reused. Such recycling minimizes environmental pollution from the surfactants and heavy metal ions. Addition of the monomer (containing initiator) to the recovered IL mixture regenerates a

*Corresponding authors. E-mail: fyan@suda.edu.cn, jtexter@emich.edu.

(1) (a) Yan, F.; Texter, J. *Soft Matter* **2006**, *2*, 109. (b) Chow, P. Y.; Gan, L. M. *Adv. Polym. Sci.* **2005**, *175*, 257. (c) Co, C. C.; de Vries, R.; Kaler, E. W. In *Reactions and Syntheses in Surfactant Systems*; Texter, J., Ed.; Marcel Dekker: New York, 2001; pp 455−469.

(2) (a) Zetterlund, P. B.; Kagawa, Y.; Okubo, M. *Chem. Rev.* **2008**, *108*, 3747. (b) Cunningham, M. F. *Prog. Polym. Sci.* **2008**, *33*, 365. (c) Cunningham, M. F. *Prog. Polym. Sci.* **2002**, *27*, 1039. (d) Qiu, J.; Charleux, B.; Matyjaszewski, K. *Prog. Polym. Sci.* **2001**, *26*, 2083.

(3) (a) Wakamatsu, J.; Kawasaki, M.; Zetterlund, P. B.; Okubo, M. *Macromol. Rapid Commun.* **2007**, *28*, 2346. (b) Zetterlund, P. B.; Nakamura, T.; Okubo, M. *Macromolecules* **2007**, *40*, 8663.

(4) Liu, S. Y.; Hermanson, K. D.; Kaler, E. W. *Macromolecules* **2006**, *39*, 4345.

(5) Apostolo, M.; Arcella, V.; Storti, G.; Morbidelli, M. *Macromolecules* **2002**, *35*, 6154.

(6) (a) Min, K.; Matyjaszewski, K. *Macromolecules* **2005**, *38*, 8131. (b) Min, K.; Gao, H.; Matyjaszewski, K. *J. Am. Chem. Soc.* **2006**, *128*, 10521. (c) Kagawa, Y.; Kawasaki, M.; Zetterlund, P. B.; Okubo, M. *Macromol. Rapid Commun.* **2007**, *28*, 2354. (d) Zetterlund, P. B.; Kagawa, Y.; Okubo, M. *Macromolecules* **2009**, *42*, 2488.

(7) (a) Matyjaszewski, K.; Pintauer, T.; Gaynor, S. *Macromolecules* **2000**, *33*, 1476. (b) Mantovani, G.; Lecolley, F.; Tao, L.; Haddleton, D. M.; Clerx, J.; Cornelissen, J.; Velonia, K. *J. Am. Chem. Soc.* **2005**, *127*, 2966. (c) Shen, Y.; Tang, H.; Ding, S. *Prog. Polym. Sci.* **2004**, *29*, 1053. (d) Ding, S.; Radosz, M.; Shen, Y. *Macromolecules* **2005**, *38*, 5921.

(8) (a) Gao, H. X.; Li, J. C.; Han, B. X.; Yan, D. D. *Phys. Chem. Chem. Phys.* **2004**, *6*, 2914. (b) Eastoe, S.; Gold, S. E.; Rogers, A.; Paul, T.; Welton, R. K.; Heenan, I. G. *J. Am. Chem. Soc.* **2005**, *127*, 7302. (c) Qiu, Z. M.; Texter, J. *J. Curr. Opin. Colloid Interface Sci.* **2008**, *13*, 252. (d) Lu, J.; Yan, F.; Texter, J. *Prog. Polym. Sci.* **2009**, *34*, 431.

**Table 1. Polymerization of MMA in [Bmim][$BF_4$]-Based Microemulsions[a]**

| entry | process | $[MMA]_0/[I]_0/[cat.]_0/[BPMOA]_0/[AIBN]_0$ | time (h) | conv (%) | $d_n$ (nm)[b] | TEM $\langle d \rangle$ (nm) | $M_n$ (g/mol) | $M_w/M_n$ |
|---|---|---|---|---|---|---|---|---|
| 1 | conventional | 100:0:0:0:1 | 4 | 64.3 | 52 | 43 ± 14 | 12 5200 | 4.89 |
| | second cycle | 100:0:0:0:1 | 4 | 63.5 | 58 | 45 ± 22 | 16 2600 | 3.73 |
| | third cycle | 100:0:0:0:1 | 4 | 64.2 | 81 | | 14 0200 | 3.40 |
| | fourth cycle | 100:0:0:0:1 | 4 | 69.1 | 66 | | 15 0400 | 2.90 |
| 2 | direct ATRP[c] | 20:1:1:2:0 | 4 | 30.2 | 79 | | 22 500 | 1.29 |
| 3 | reverse ATRP[d] | 20:0:1:2:1 | 18.5 | 38.5 | 39 | 44 ± 14 | 17 400 | 1.28 |
| | second cycle | 20:0:1:2:1 | 18.5 | 34.3 | 62 | 38 ± 21 | 16 200 | 1.26 |
| | third cycle | 20:0:1:2:1 | 18.5 | 41.2 | 65 | 62 ± 17 | 17 100 | 1.19 |
| | fourth cycle | 20:0:1:2:1 | 18.5 | 35.5 | 66 | | 16 700 | 1.29 |

[a] The reaction temperature was 60 °C for conventional free radical polymerization, 70 °C for direct ATRP, and 90 °C for reverse ATRP; the weight ratio of surfactant to monomer is 3 for all polymerizations. [b] Number-average diameter ($d_n$) of PMMA particles measured by dynamic light scattering. [c] The initiator and catalyst for ATRP were ethyl 2-bromoisobutyrate (EBiB) and CuCl, respectively. [d] The catalyst for reverse ATRP was $CuCl_2$.

microemulsion suitable for another polymerization cycle (Figure 1). We also demonstrate that such recycling produces good batch-to-batch reproducibility.

As the first demonstration of this approach, a conventional free radical polymerization of methyl methacrylate (MMA) was conducted in a 1-butyl-3-methylimidazolium tetrafluoroborate ([Bmim][$BF_4$])-based microemulsion stabilized by 1-dodecyl-3-methylimidazolium bromide (DMIBr). DMIBr is also an IL with $T_m$ = 39.7 °C.[9] An MMA/[Bmim][$BF_4$]/DMIBr ternary phase diagram is illustrated in the Supporting Information (Figure S1). Samples within the one-phase microemulsion region were transparent and stable. Polymerization of MMA was initiated thermally using AIBN. The transparency of the microemulsion decreased after about 5 min as indicated by the appearance of a bluish color, indicating that polymerization had started. After the completion of the polymerization, the reaction mixture was added dropwise to a large amount of methanol. The precipitated PMMA was isolated by filtration and washed with methanol. It is not surprising that either PMMA latexes with ~52 nm diameter (according to the dynamic light scattering (DLS) measurements) or bicontinuous nanostructures were produced, depending on the microemulsion formulations (Table 1, entry 1). These results are similar to those for polymerizations conducted in aqueous microemulsions.

The IL surfactant, DMIBr, is miscible with [Bmim][$BF_4$] and methanol. Therefore, it is quite easy to separate from the resultant polymers. After the evaporation of methanol and any residual monomer in vacuo, the mixture of ILs (continuous phase IL and surfactant) was recovered. The addition of a proper amount of monomer (containing initiator) to the recovered IL mixture regenerated a transparent, stable microemulsion. Under the same experimental polymerization conditions, the recovered IL-based microemulsion produced polymers with reproducible particle size (Table 1, entry 1). It is interesting that the molecular weight dispersity of PMMA decreases as the number of cycles increases from 4.89 to 2.90 over four cycles (Figure 2). The purity of the ionic liquid used in this work was confirmed by NMR. However, we believe that there is still some impurity, such as residual bromobutane used for the synthesis of ionic liquid, that may act as a chain-transfer agent and therefore broaden the molecular-weight dispersity. Such an impurity would gradually be consumed during the polymerization and thus lower the molecular weight dispersity with an increasing number of cycles.

Direct ATRP in such an IL-based microemulsion was carried out as described in Table 1, entry 2, where ethyl-2-bromoisobutyrate (EBiB) as the initiator was added to the MMA/[Bmim][BF4]/DMIBr microemulsion with CuCl and *N*-bis(2-pyridylmethyl)-octylamine (BPMOA). The color changed from yellow to yellow-green and then to green in a few minutes, and the microemulsion turned slightly translucent, indicating fast nucleation. The final latexes appeared to be a gel-like liquid with particles of ~79 nm and low molecular-weight polydipsersity ($M_w/M_n$ = 1.29), indicating excellent control (Supporting Information, Figure S4).

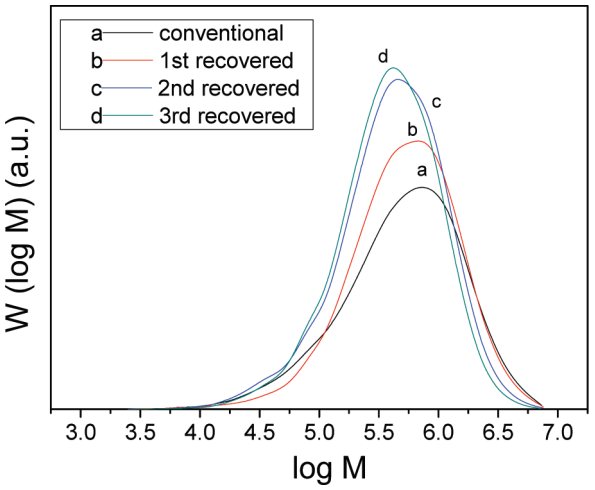


**Figure 2.** Typical GPC traces of the PMMA from conventional radical polymerization in a [Bmim] [$BF_4$]-based microemulsion (as described in Table1, entry 1).

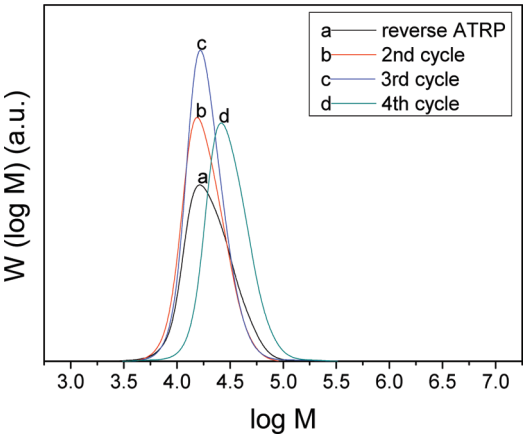


**Figure 3.** Typical GPC traces of PMMA from reverse ATRP in a [Bmim] [$BF_4$]-based microemulsion (as described in Table 1, entry 3).

(9) (a) Yan, F.; Texter, J. *Angew. Chem., Int. Ed.* **2007**, *46*, 2440. (b) Yan, F.; Texter, J. *Chem. Commun.* **2006**, 2696. (c) Yu, S.; Yan, F.; Zhang, X.; You, J.; Wu, P.; Lu, J.; Xu, Q.; Xia, X.; Ma, G. *Macromolecules* **2008**, *41*, 3389. (d) Yan, F.; Yu, S.; Zhang, X.; Qiu, L.; Chu, F.; You, J.; Lu, J. *Chem. Mater.* **2009**, *21*, 1480.

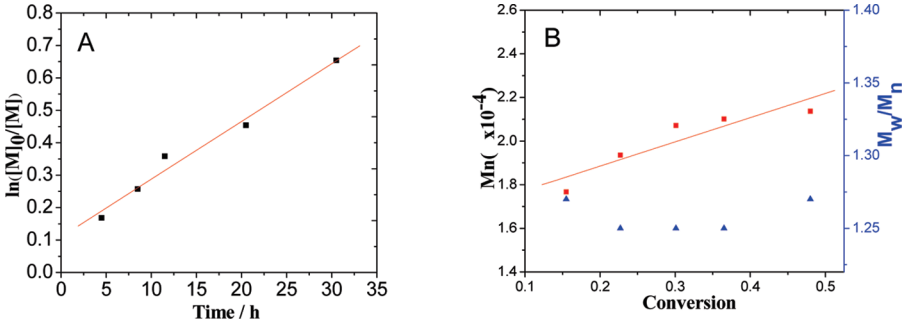


**Figure 4.** (A) First-order rate plots and (B) dependence of Mn on the monomer conversion for the reverse ATRP of MMA conducted in an IL-microemulsion at 90 °C. Conditions: $[MMA]_0/[CuCl_2]_0/[BPMOA]_0/[AIBN]_0 = 20:1:2:1$.

**Table 2. Effect of Ligands on [Bmim][$BF_4$]-Based Microemulsion Reverse ATRP[a]**

| monomer | ligand | ligand solubility in [Bmim][ $BF_4$] (wt %) | time (h) | conv (%) | $d_n$ (nm) | $M_n$ (g/mol) | $M_w/M_n$ |
|---|---|---|---|---|---|---|---|
| MMA | bipy | miscible | 24 | 0 | | no reaction | |
| MMA | PMEDTA | 22 | 24 | 8.2 | | bimodal | |
| MMA | $MA_5$EDTA | 13 | 3 | 51.4 | | 31 300 | 1.54 |
| MMA | BPMOA | 2.5 | 18.5 | 38.5 | 39 | 17 400 | 1.28 |
| styrene | $MA_5$EDTA | 13 | 3 | 25.5 | 94 | 8800 | 1.55 |

[a] The reaction temperature was 90 °C and $[M]_0/[CuCl_2]_0/[ligand]_0/[AIBN]_0 = 20:1:2:1$ for all polymerizations.

However, the Cu(I) catalysts used for direct ATRP are easily oxidized, which requires anaerobic processing. This limitation can be avoided by using reverse ATRP, where the catalyst Cu(II) complex is not air-sensitive. Reverse ATRP of MMA in an IL-based microemulsion was conducted as described in Table 1, entry 3. After the decomposition of radical initiator AIBN, Cu(I) activator complexes were formed and the microemulsion color changed from green to brown. The resulting polymer was precipitated and washed with methanol. This reverse ATRP was well controlled as evidenced by molecular weight $M_n$ = 17 400 g/mol with low molecular-weight dispersity, $M_w/M_n$ = 1.28. Microemulsion reverse ATRP systems are also recyclable. The addition of monomer (containing initiator) to the recovered ionic liquids regenerates a transparent, stable microemulsion in which a second reverse ATRP cycle was carried out. Although no extra catalyst, ligand, or surfactant was added, higher catalytic activity and similar control over polymerization were observed. Reverse ATRP of MMA in recovered microemulsions produced PMMA with reproducible molecular weight, narrow molecular-weight polydispersity, and particle size, even in the fourth cycle (Figure 3).

Figure 4A shows the kinetic plots of $\ln([M]_0/[M])$ versus time for reverse ATRP of MMA in an IL-microemulsion. The linearity of the plot indicates that the polymerization was approximately first order with respect to the monomer concentration. The slope of the kinetic plots indicates that the number of active species was constant and the termination reactions could be neglected throughout the polymerization process. The molecular weight increased linearly with conversion, and the molecular weight distributions were narrow, $M_w/M_n < 1.3$ up to 50% conversion (Figure 4B). These results indicate that the reaction proceeded as a well-controlled polymerization process.

However, the obtained molecular weight of PMMA was much higher than those predicted for quantitative initiation, and the initiation efficiency was low in this work. It has been demonstrated by Matyjaszewski and co-workers that the nucleation period in reverse ATRP was relatively longer than that in direct ATRP because of the slow decomposition of the AIBN conventional radical initiator.[6a] The calculated half-lifetime of AIBN at 90 °C is about 40 min.[10a] This slow decomposition led to slow initiation that resulted in a low overall initiator efficiency and a higher molecular weight of the polymers than theoretical values. However, the low initiation efficiency might as well be simply due to the solubility of AIBN and $CuCl_2$ in [Bmim][$BF_4$], which was uncomplexed by BPMOA. Being excellent radical scavengers, these Cu(II) salts likely terminate radicals in the ionic liquid phase but do not reinitiate the polymerization in micelles, thereby reducing the overall initiator efficiency.[10b] To improve the reverse ATRP initiation efficiency, higher operating termperatures and greater catalyst-to-initiator ratios are needed.

Compared with reverse ATRP in aqueous microemulsions reported previously,[6a] a relatively high concentration of catalyst was used in this work. In part, this was due to the good solubility of the catalyst complex in the ionic liquid continuous phase. FTIR, NMR, and XPS spectra characterization confirmed that the produced polymers were not contaminated significantly with ionic liquid, surfactant, or copper catalyst (Supporting Information, Figures S2 and S3). Inductively coupled plasma (ICP) measurements showed that the residual concentration of copper catalyst in the produced polymers was in the range of 49−85 ppm, indicating that most of the catalyst had been effectively separated, although no special purification treatments were applied.

For well-controlled microemulsion reverse ATRP, the selection of a ligand for the formation of the catalyst complex is crucial for maintaining an appropriate equilibrium of the activator and the deactivator between the organic monomer-swollen micelles and the IL pseudocontinuous phase.[11] When 2,2′-bipyridine (bipy), which is miscible with [Bmim][$BF_4$], was used as a ligand, no polymerization was observed (Table 2). In cases in which *N*,*N*,*N*′,*N*″,*N*‴-pentamethyl-diethylentriamine (PMEDTA) or *N*,*N*,*N*′,*N*′,*N*″-penta(methyl acrylate)-diethylenetriamine ($MA_5$-DETA), each having high solubility in [Bmim][$BF_4$], was selected, bimodal or broader MWDs in GPC traces were observed. However, BPMOA is nearly insoluble in [Bmim][$BF_4$], and when it was

(10) (a) Moad, G.; Solomon, D. H. *The Chemistry of Free Radical Polymerization*; Pergamon: Oxford, U.K., 1995.(b) Qiu, J.; Gaynor, S. G.; Matyjaszewski, K. *Macromolecules* **1999**, *32*, 2872.

(11) (a) Qiu, J.; Shipp, D.; Gaynor, S. G.; Matyjaszewski, K. *Polym. Prepr.* **1999**, *40*, 418. (b) Biedron, T.; Kubisa, P. *Macromol. Rapid Commun.* **2001**, *22*, 1237.

used as a catalyst ligand, it resulted in well-controlled polymerization.

In summary, we have presented the first examples of direct and reverse ATRP in monomer/IL microemulsions stabilized by IL surfactants. Furthermore, we have shown that with the appropriate selection of recovery solvent (immiscible with product polymer and miscible with ILs), chain polymerization and reverse ATRP can very effectively be continued in recycled microemulsions. After the completion of polymerization, ILs (continuous phase and surfactants) and catalysts can be simply recovered and reused. The addition of immiscible monomer to the recovered IL mixture regenerates transparent, stable microemulsions. Further addition of initiator produces polymers with reproducible particle size, well-controlled molecular weight, and low polydispersity. The method combines the advantages of IL recycling and microemulsion polymerization. Although only polymerizations in IL-based microemulsion were studied in this work, we believe that this strategy could be extended to other heterogeneous systems, such as emulsion polymerization and miniemulsion suspension polymerization using IL-based continuous phases.

**Acknowledgment.** This work was supported by the NSFC (grant nos. 20974072 and 20874071), the Program for New Century Excellent Talents in University (grant no. NCET-07-0593), and the Fok Ying Tung Education Foundation (grant no. 114022). J.T. gratefully acknowledges the support of AFOSR (grant no. FA9550-08-1-0431) and the hospitality of Professor Markus Antonietti and the Max Planck Society during his sabbatical leave in Golm.

**Supporting Information Available:** Experimental details of microemulsion polymerization and characterization. This material is available free of charge via the Internet at http://pubs.acs.org.

# Supporting Information

## Sustainable Polymerizations in Recoverable Microemulsions

### 1. Materials

Methyl methacrylate (MMA) and sytrene were made inhibitor-free by passing the liquid through a column filled with $Al_2O_3$. The radical initiator, 2,2-azobisisobutyronitrile (AIBN) was recrystallized from ethanol and dried at room temperature under vacuum. Methanol, diethyl ether, ethyl acetate were used as received. Distilled deionized water was used for all experiments. [Bmim][$BF_4$] was freshly synthesized and further dehydrated as documented in the literature.[1] Surfactant, 1-dodecyl-3-methylimidazolium bromide (DMIB) was synthesized as described in the literature.[2] Ethyl 2-bromoisobutyrate (EBiB) was used as received without any further purification. $CuCl_2$ was dried at 80 $^oC$ for 24 h before use. CuCl was purified according to the literature.[3] Bis(2-pyridylmethyl)octylamine (BPMOA) was synthesized as reported in the literature.[4] *N,N,N′,N′,N″*-penta(methyl acrylate) diethylenetriamine ($MA_5$-DETA) was prepared according to the procedures previously published.[5]

### 2. Microemulsion Polymerization

#### 2.1 Conventional Microemulsion Polymerization

The MMA/[Bmim][$BF_4$]/DMIB microemulsion was bubbled with nitrogen for 15 min and then heated to 60 $^oC$. After the completion of the polymerization, the reaction was stopped by immersing in the ice bath, and then pouring into the methanol. The precipitated polymers were isolated by filtration and washed with methanol.

#### 2.2 Direct ATRP in Microemulsion

Microemulsion containing CuCl, BPMOA, MMA, [Bmim][$BF_4$] and DMIB was stirred under nitrogen atmosphere and cooled with an ice bath. After the subsequent addition of EBiB, the resulting transparent microemulsion was degassed with several $N_2$ cycles and sealed off. The

reaction mixture was then heated to 70 $^{o}$C. After the completion of the polymerization, the microemulsion ATRP was stopped by immersing in an ice bath and then pouring into the methanol. The precipitated polymers were isolated by filtration and washed with methanol.

**2.3 Reverse ATRP in Microemulsion.**

Typical reverse ATRP procedure: microemulsion containing $CuCl_2$, BPMOA, MMA, [Bmim][$BF_4$], AIBN and DMIB was degassed by three freeze–pump–thaw cycles vacuo and was sealed under nitrogen. The reaction was then heated to 90 $^{o}$C. After the completion of the polymerization, the reaction mixture was stopped by immersing in an ice bath and then pouring into the methanol. The precipitated polymers were isolated by filtration and washed with methanol.

**3. Characterization**

$^{1}$H NMR spectra were recorded on a UNITY INOVA 400 spectrometer. Gel permeation chromatography (GPC) was conducted on Waters 1515 to determine polymer molecular weights and molecular weight distributions using tetrahydrofuran (THF) as eluent at 30 °C. The residue copper concentration in the resultant polymers was measured by inductively coupled plasma (ICP) (Vista MPX). The polymer powder (50.0 mg) was dissolved in nitric acid with heating and was then diluted to 25 ml for ICP analysis. The dynamic light scattering measurements were performed using a high performance particle size HPPS 5001 autosizer (Malvern Instrument, U.K.). Transmission electron microscopy (TEM) characterization was performed on a JEOL JEM-2010 electron microscope operating at an acceleration voltage of 200 kV.

## 4. Partial Phase Diagrams

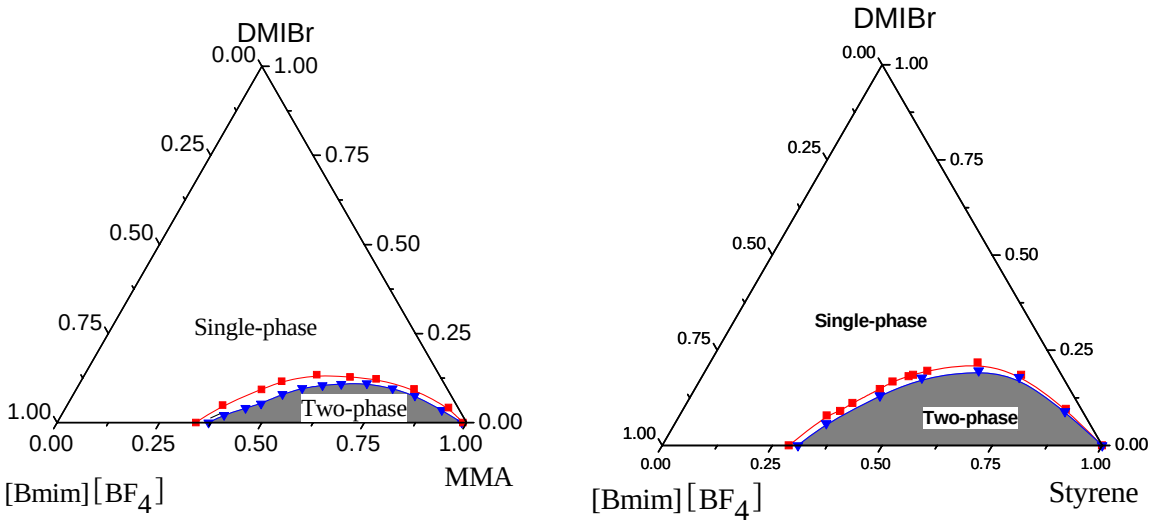


**Figure S1**. Partial phase diagrams (weight fraction) of DMIBr/[Bmim] [$BF_4$]/MMA (left), and DMIBr/[Bmim] [$BF_4$]/styrene (right) systems at 25°C (blue line) and 90 °C (red line). A few parts per million of 1,4-dihydroxybenzene was added to inhibit thermal polymerization.

## 5. XPS and NMR spectra of resultant PMMA nanoparticles

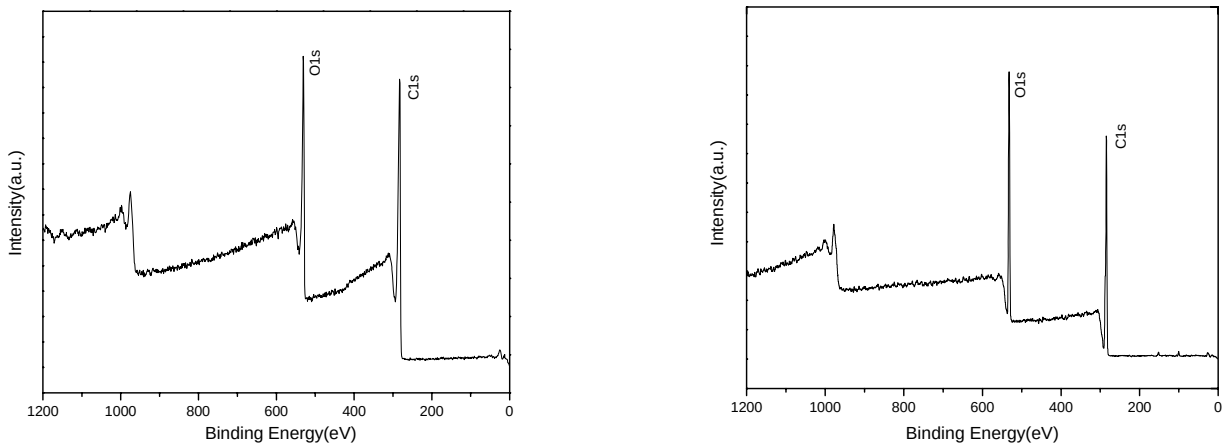


**Figure S2**. XPS spectra of resultant PMMA nanoparticles obtained from conventional polymerization (left); and reverse ATRP (right ) in IL-based microemulsion. There is no trace of N(1s) in the neighborhood of 399-401 eV or of Br(3d) close to 60-69 eV as reported by Park et al.[6] in their XPS analyses of imidazolium bromide surface functionalized nanodiamond particles or by Roh [7] in a study of imidazolium bromide stabilized MWCNTs.

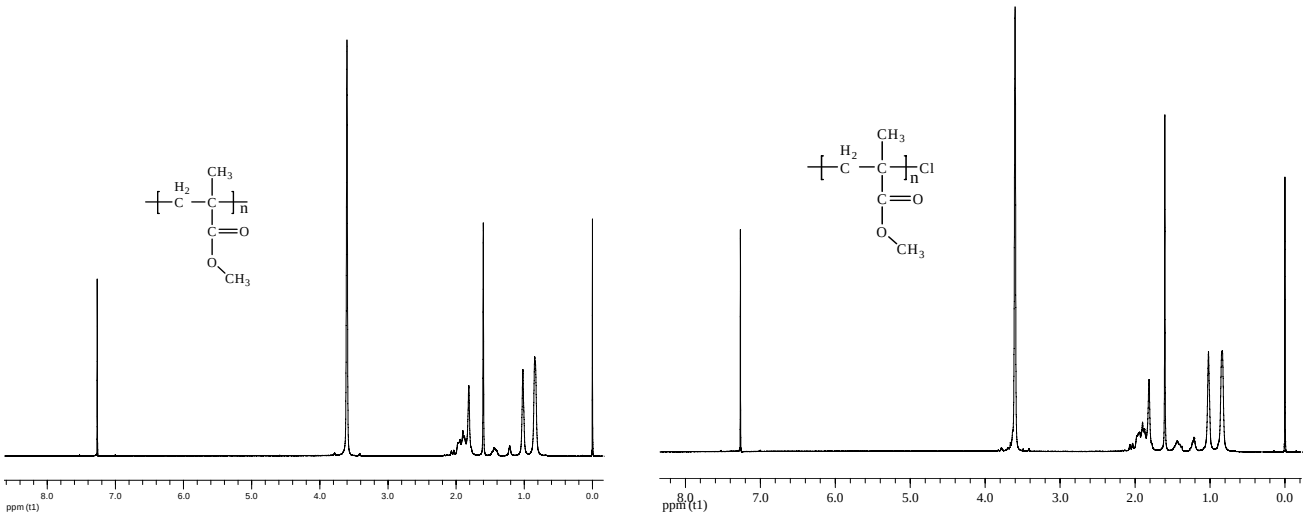


**Figure S3**. $^{1}$HNMR spectra of resultant PMMA nanoparticles obtained from conventional polymerization (left) and reverse ATRP (right ) conducted in IL-based microemulsion. The residual surfactant was not detected.

## 6. GPC of PMMA and PS from IL-based Microemulsions

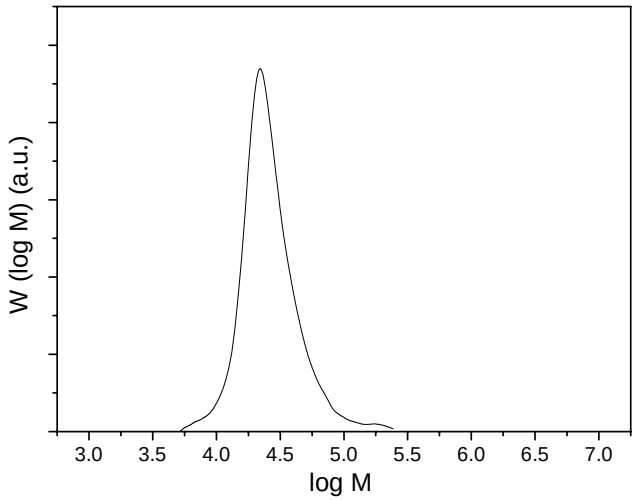


**Figure S4**. Typical GPC traces of the PMMA from direct ATRP in [Bmim] [$BF_4$]-based microemulsion (as described in Table1, Entry 2).

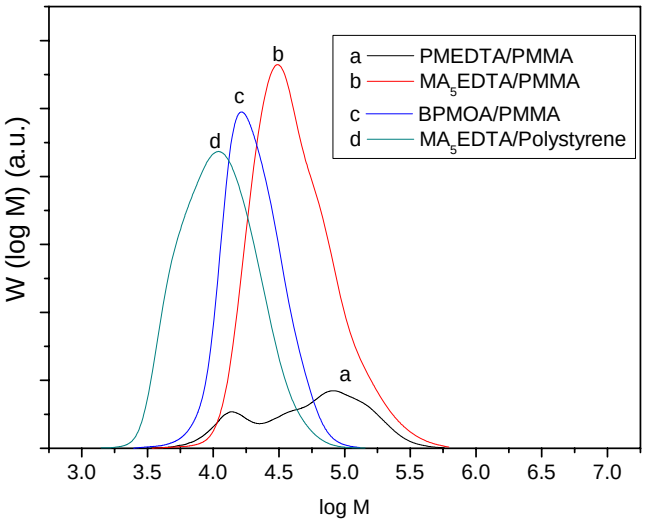


**Figure S5**. Typical GPC traces of the PMMA (curves a, b, c) and polystyrene (cure d) from reverse ATRP in [Bmim] [$BF_4$]-based microemulsion with different ligand (as described in **Table 2**).

## 7. Particle size of PMMA from IL-based Microemulsions

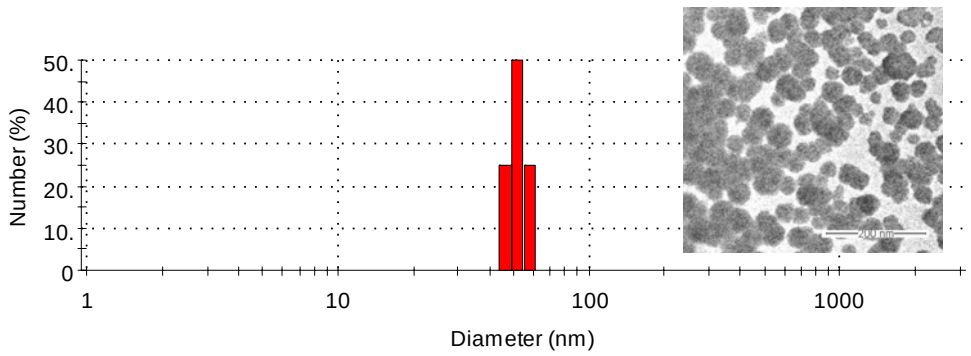


**Figure S6**. Particle size and particle size distribution of PMMA produced via Conventional polymerization in IL-based microemulsion (**Table1 entry 1**).Inset shows a TEM imageof the PMMA particles.

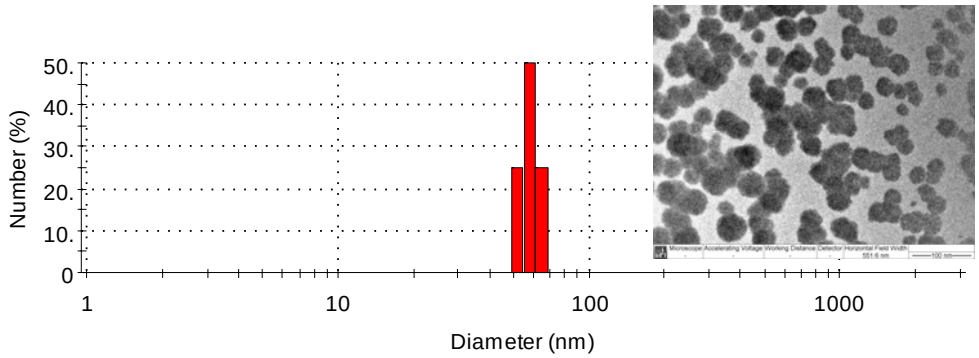


**Figure S7**. Particle size and particle size distribution of PMMA produced via conventional polymerization in IL-based microemulsion (**Table1 entry 1, 2nd cycle**). Inset shows a TEM imageof the PMMA particles.

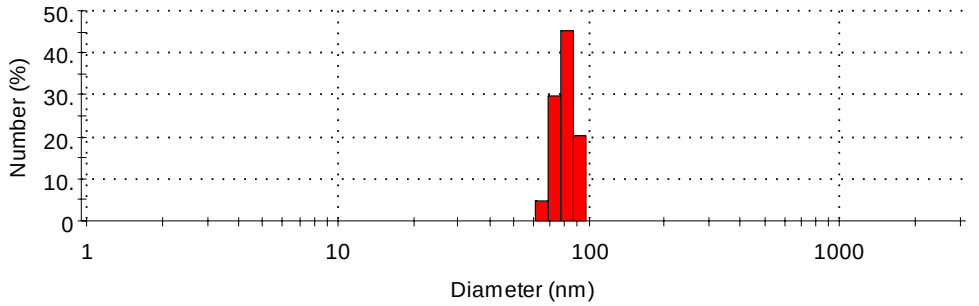


**Figure S8**. Particle size and particle size distribution of PMMA produced via conventional polymerization in IL-based microemulsion (**Table1 entry 1, 3rd cycle**).

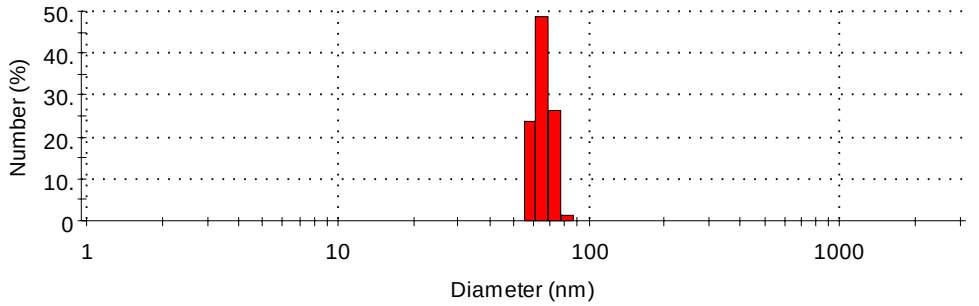


**Figure S9**. Particle size and particle size distribution of PMMA produced via conventional polymerization in IL-based microemulsion (**Table1 entry 1, 4th cycle**).

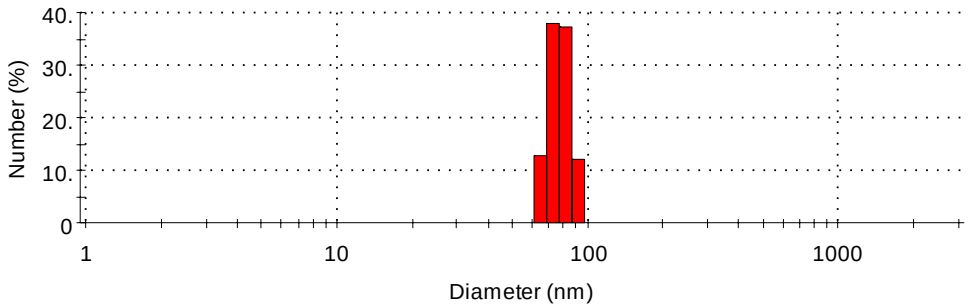


**Figure S10**. Particle size and particle size distribution of PMMA produced via ATRP polymerization in IL-based microemulsion (**Table1 entry 2**).

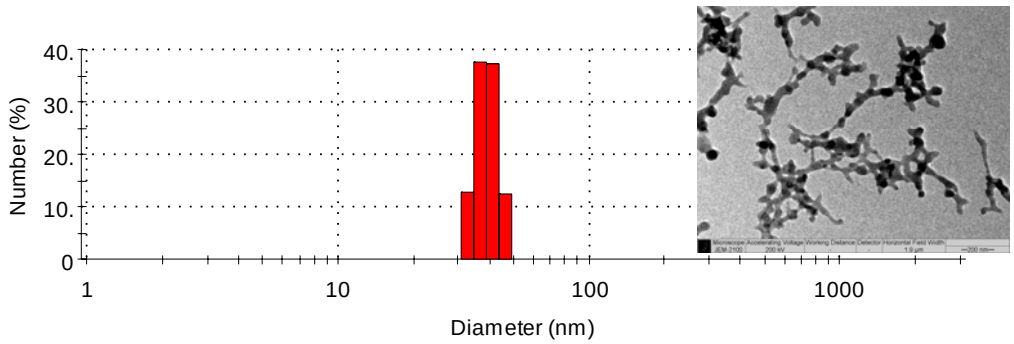


**Figure S11**. Particle size and particle size distribution of PMMA produced via everse ATRP polymerization in IL-based microemulsion (**Table1 entry 3**). Inset shows a TEM image of the PMMA particles.

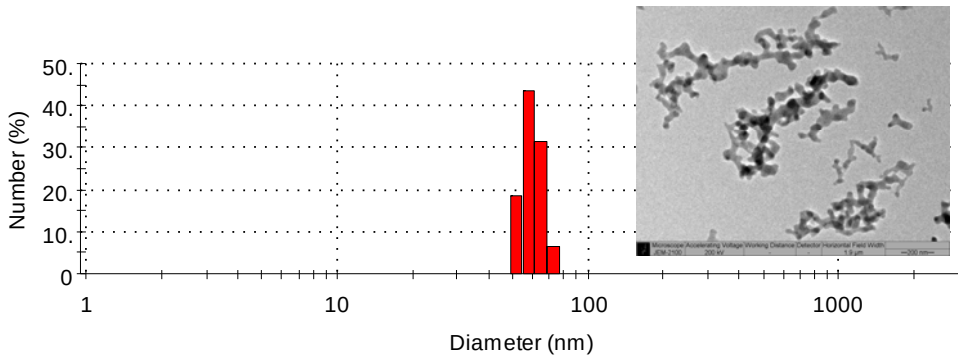


**Figure S12**. Particle size and particle size distribution of PMMA produced via reverse ATRP polymerization in IL-based microemulsion (**Table1 entry 3, 2$^{nd}$ cycle**). Inset shows a TEM image of the PMMA particles.

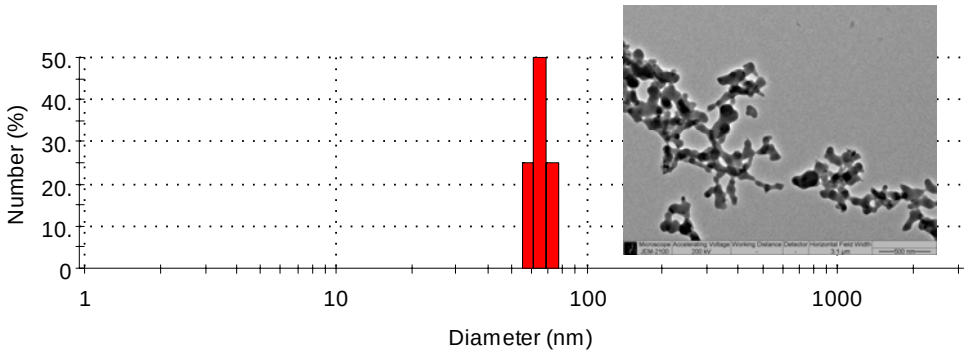


**Figure S13**. Particle size and particle size distribution of PMMA produced via reverse ATRP polymerization in IL-based microemulsion (**Table1 entry 3, 3rd cycle**). Inset shows a TEM image of the PMMA particles.

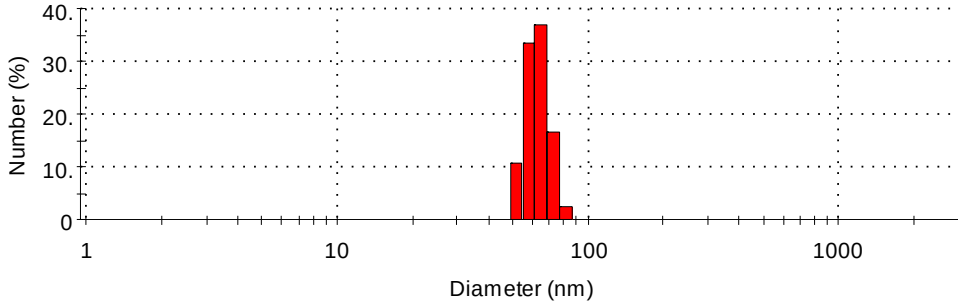


**Figure S14**. Particle size and particle size distribution of PMMA produced via reverse ATRP polymerization in IL-based microemulsion (**Table1 entry 3, 4th cycle**).

## References

[1] Rivera-Rubero, S.; Baldelli, S. *J. Phys. Chem. B*, **2006,** *110,* 4756.

[2] Yan, F.; Texter, J. *Chem. Comm.*, **2006**, 2696.

[3] Keller, R. N.; Wycoff, H. D. *Inorg Synth.*, **1946**, *2*, 1

[4] Xia, J.; Matyjaszewski, K. *Macromolecules*, **1999**, *32*, 2434.

[5] Chu, J.; Chen, J.; Zhang, K. D. *J. Polym. Sci.: Part A: Polym. Chem.*, **2004**, *42*, 1963.

[6] Park, C, L.; Jee, A. Y.; Lee, M. Y.; Lee, S. G. *Chem. Comm.*, **2009**, 5576.

[7] Roh, E. J.; Final Report for AFOSR Contract Number: AOARD-05-4077, June 23, 2006; http://handle.dtic.mil/100.2/ADA455944; downloaded September 27, 2009.